

 Open access • Posted Content • DOI:10.1101/2020.05.13.093195

ChAdOx1 nCoV-19 vaccination prevents SARS-CoV-2 pneumonia in rhesus macaques.

— [Source link](#) 

Neeltje van Doremalen, Teresa Lambe, Alexandra J. Spencer, Sandra Belij-Rammerstorfer ...+32 more authors

Institutions: National Institutes of Health, University of Oxford

Published on: 13 May 2020 - bioRxiv (Cold Spring Harbor Laboratory)

Topics: Vaccination, Immunogenicity, Viral load, Immune system and Bronchoalveolar lavage

Related papers:

- [Development of an inactivated vaccine candidate for SARS-CoV-2.](#)
- [ChAdOx1 nCoV-19 vaccine prevents SARS-CoV-2 pneumonia in rhesus macaques.](#)
- [DNA vaccine protection against SARS-CoV-2 in rhesus macaques.](#)
- [Cryo-EM structure of the 2019-nCoV spike in the prefusion conformation.](#)
- [SARS-CoV-2 Cell Entry Depends on ACE2 and TMPRSS2 and Is Blocked by a Clinically Proven Protease Inhibitor](#)

Share this paper:    

View more about this paper here: <https://typeset.io/papers/chadox1-ncov-19-vaccination-prevents-sars-cov-2-pneumonia-in-3f79yohab4>

1 **ChAdOx1 nCoV-19 vaccination prevents SARS-CoV-2 pneumonia in rhesus macaques**

2
3 Neeltje van Doremalen^{1*}, Teresa Lambe^{2*}, Alexandra Spencer², Sandra Belij-Rammerstorfer²,
4 Jyothi N. Purushotham^{1,2}, Julia R. Port¹, Victoria Avanzato¹, Trenton Bushmaker¹, Amy
5 Flaxman², Marta Ulaszewska², Friederike Feldmann³, Elizabeth R. Allen², Hannah Sharpe²,
6 Jonathan Schulz¹, Myndi Holbrook¹, Atsushi Okumura¹, Kimberly Meade-White¹, Lizzette
7 Pérez-Pérez¹, Cameron Bissett², Ciaran Gilbride², Brandi N. Williamson¹, Rebecca Rosenke³,
8 Dan Long³, Alka Ishwarbhai², Reshma Kailath², Louisa Rose², Susan Morris², Claire Powers²,
9 Jamie Lovaglio³, Patrick W. Hanley³, Dana Scott³, Greg Saturday³, Emmie de Wit¹, Sarah C.
10 Gilbert^{2#}, Vincent J. Munster^{1#}.

11
12 *1. Laboratory of Virology, National Institute of Allergy and Infectious Diseases, National*

13 *Institutes of Health, Hamilton, MT, USA.*

14 *2. The Jenner Institute, University of Oxford, Oxford, UK*

15 *3. Rocky Mountain Veterinary Branch, National Institute of Allergy and Infectious*

16 *Diseases, National Institutes of Health, Hamilton, MT, USA*

17
18 *Joint first authors

19 #Joint senior authors

20 **Severe acute respiratory syndrome coronavirus-2 (SARS-CoV-2) emerged in December**
21 **2019^{1,2} and is responsible for the COVID-19 pandemic³. Vaccines are an essential**
22 **countermeasure urgently needed to control the pandemic⁴. Here, we show that the**
23 **adenovirus-vectored vaccine ChAdOx1 nCoV-19, encoding the spike protein of SARS-**
24 **CoV-2, is immunogenic in mice, eliciting a robust humoral and cell-mediated response.**
25 **This response was not Th2 dominated, as demonstrated by IgG subclass and cytokine**
26 **expression profiling. A single vaccination with ChAdOx1 nCoV-19 induced a humoral and**
27 **cellular immune response in rhesus macaques. We observed a significantly reduced viral**
28 **load in bronchoalveolar lavage fluid and respiratory tract tissue of vaccinated animals**
29 **challenged with SARS-CoV-2 compared with control animals, and no pneumonia was**
30 **observed in vaccinated rhesus macaques. Importantly, no evidence of immune-enhanced**
31 **disease following viral challenge in vaccinated animals was observed. ChAdOx1 nCoV-19 is**
32 **currently under investigation in a phase I clinical trial. Safety, immunogenicity and efficacy**
33 **against symptomatic PCR-positive COVID-19 disease will now be assessed in randomised**
34 **controlled human clinical trials.**

35

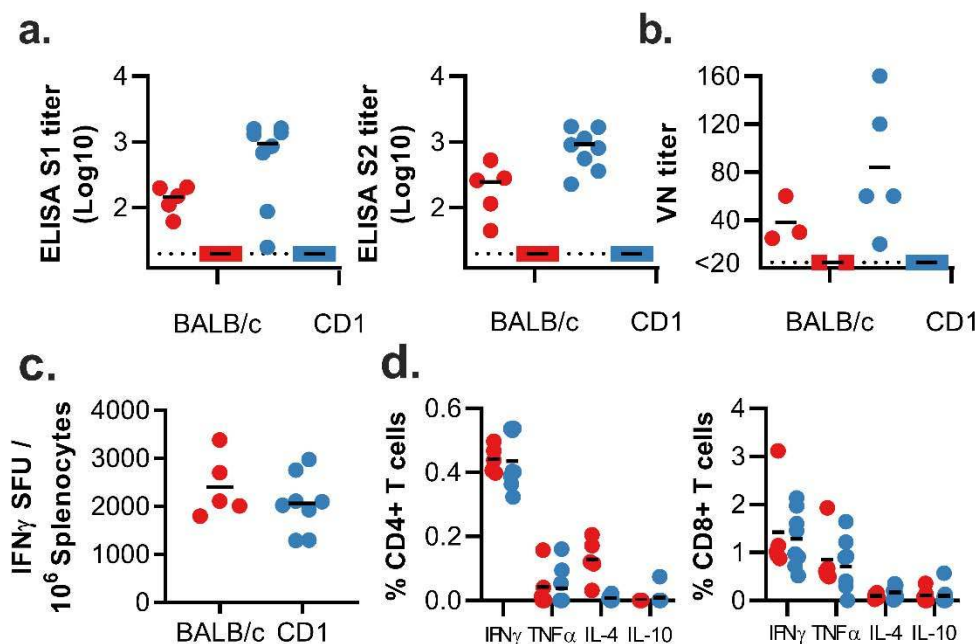
36 **Main**

37 We previously demonstrated that a single dose of ChAdOx1 MERS, a chimpanzee adeno
38 (ChAd)-vectored vaccine platform encoding the spike protein of MERS-CoV, protected non-
39 human primates (NHPs) against MERS-CoV-induced disease⁵. Here, we designed a ChAdOx1-
40 vectored vaccine encoding a codon-optimised full-length spike protein of SARS-CoV-2
41 (YP_009724390.1) with a human tPA leader sequence, provisionally named ChAdOx1 nCoV-
42 19, similar to the approach for ChAdOx1 MERS⁵.

43

44 **Immunogenicity in mice**

45 Two mouse strains (BALB/c, N=5 and outbred CD1, N=8) were vaccinated intramuscularly (IM)
46 with ChAdOx1 nCoV-19 or ChAdOx1 GFP, a control vaccine expressing green fluorescent
47 protein. Humoral and cellular immunity were studied 9-14 days later. Total IgG titers were
48 detected against spike protein subunits S1 and S2 in all vaccinated mice (Figure 1a). Profiling of
49 the IgG subclasses showed a predominantly Th1 response post vaccination (Extended Data
50 Figure 1a). Virus-specific neutralising antibodies were detected in all mice vaccinated with
51 ChAdOx1 nCoV-19, whereas no neutralisation was detected in serum from mice vaccinated with
52 ChAdOx1 GFP (Figure 1b). Splenic T-cell responses measured by IFN- γ ELISpot and
53 intracellular cytokine staining (ICS) were detected against peptides spanning the full length of
54 the spike construct (Figure 1c). Again, a strong Th1-type response was detected post vaccination
55 as supported by high levels of IFN- γ and TNF- α , and low levels of IL-4 and IL-10 (Figure 1d &
56 Extended Data Figure 1b-c).



57

58 **Figure 1: Humoral and cellular immune responses to ChAdOx1 nCoV-19 vaccination in**
59 **mice.**

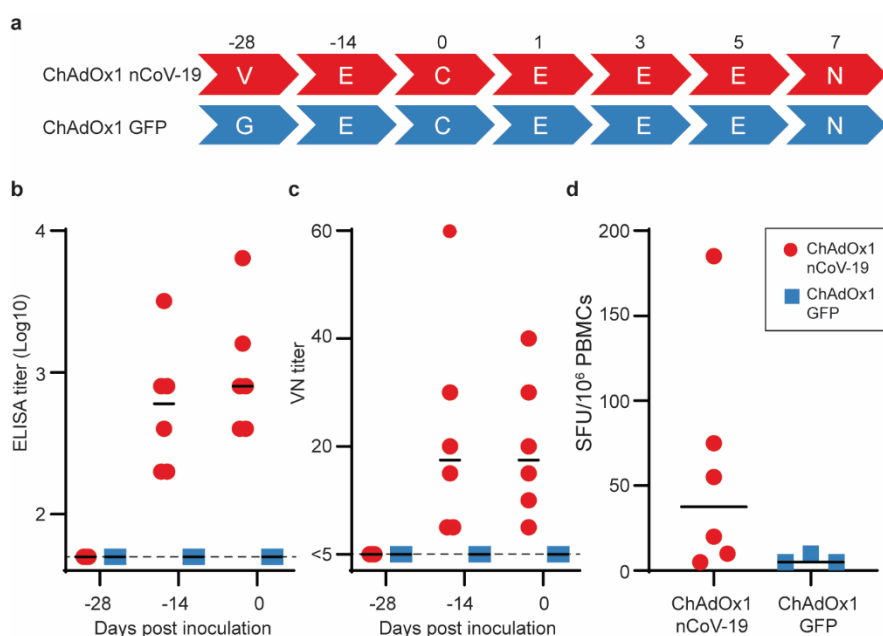
60 a. End point titer of serum IgG detected against S1 or S2 protein. Control mice were below the
61 limit of detection. b. Virus neutralizing titer in serum. c. Summed IFN- γ ELISpot responses in
62 splenocytes toward peptides spanning the spike protein. Control mice had low (<100 SFU) or no
63 detectable response. d. Summed frequency of spike-specific cytokine positive CD4+ or CD8+ T
64 cells. BALB/c = red; CD1 = blue; vaccinated = circle; control = square; dotted line = limit of
65 detection; line = mean; SFU = spot-forming units.

66

67 **Immunogenicity in rhesus macaques**

68 We next evaluated the efficacy of ChAdOx1 nCoV-19 in rhesus macaques, a non-human primate
69 model that displays robust infection of upper and lower respiratory tract and virus shedding upon
70 inoculation with SARS-CoV-2⁶. Twenty-eight days before challenge, 6 animals were vaccinated

71 intramuscularly with 2.5×10^{10} ChAdOx1 nCoV-19 virus particles each, half of the dose
72 currently administered in human clinical trials. As a control, three animals were vaccinated via
73 the same route with the same dose of ChAdOx1 GFP (Figure 2a). Spike-specific antibodies were
74 present as early as 14 days post vaccination and endpoint IgG titers of 400-6400 were measured
75 on the day of challenge (Figure 2b). Virus-specific neutralising antibodies were detectable in all
76 vaccinated animals before challenge (VN titer = 5-40), whereas no virus-specific neutralising
77 antibodies were detected in control animals (Figure 2c). Finally, SARS-CoV-2 spike specific T-
78 cell responses were detected by IFN- γ ELISpot assay and involved stimulation of peripheral
79 blood mononuclear cells (PBMCs) with a peptide library spanning the full length of the spike
80 protein (Figure 2d).



81
82 **Figure 2. Humoral and cellular immune responses to ChAdOx1 nCoV-19 vaccination in**
83 **rhesus macaques.**

84 a. Study schedule for NHPs. V = vaccination with ChAdOx1 nCoV-19; G = vaccination with
85 ChAdOx1 GFP; E = exam; N = exam and necropsy. b. Virus neutralizing titer in serum. d.

86 Summed IFN- γ ELISpot responses in PBMCs toward peptides spanning the spike protein
87 Vaccinated animals = red circles; control animals = blue squares; dotted line = limit of detection;
88 line – median; SFU = spot-forming units.

89

90 **Clinical signs**

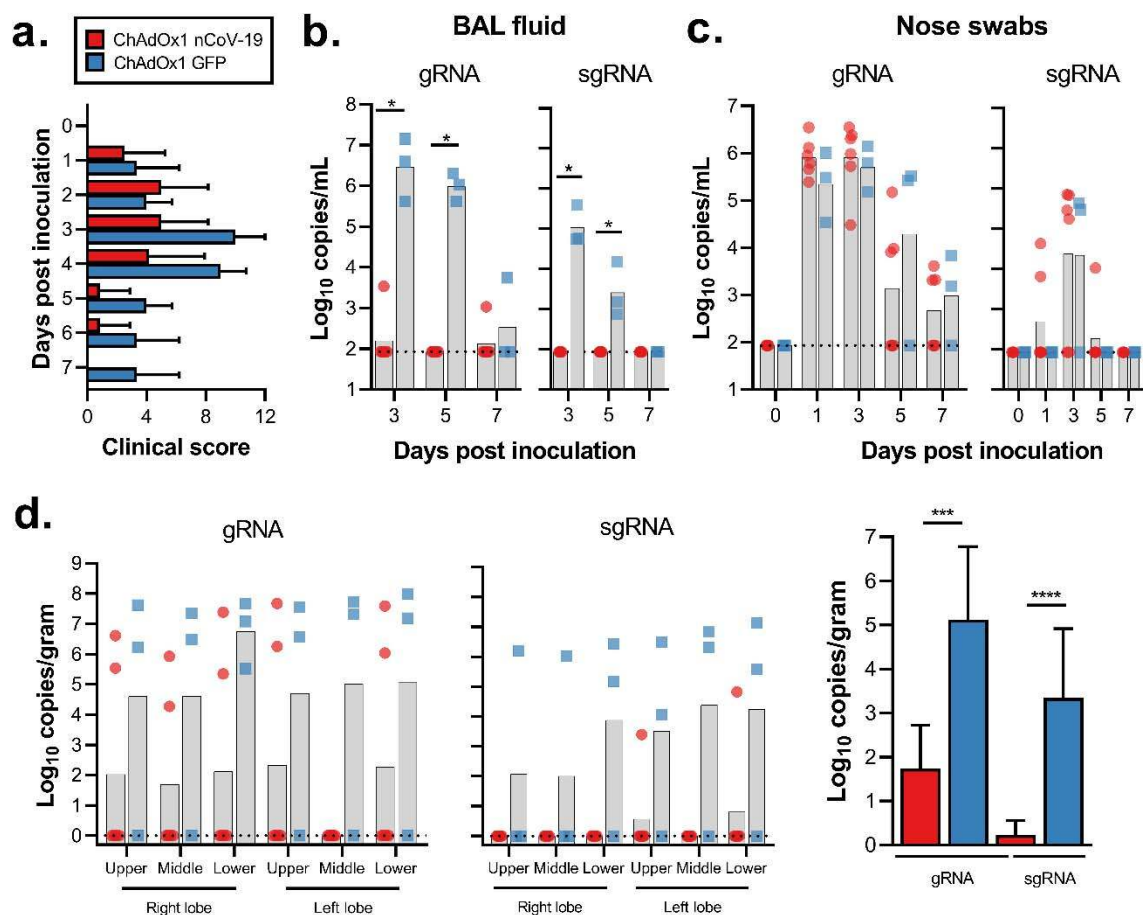
91 Upon challenge with 2.6×10^6 TCID₅₀ SARS-CoV-2 to both the upper and lower respiratory
92 tract the average clinical score of control animals was higher compared to ChAdOx1 nCoV-19
93 vaccinated animals. This was significantly different as determined via Mann-Whitney's rank's
94 test on 3 and 5 DPI (Figure 3a). All control animals showed an increase in respiratory rate,
95 compared to 3 out of 6 vaccinated animals. Respiratory signs persisted longer in control animals
96 (Extended Data Table 1).

97

98 **Viral load in respiratory tract samples**

99 In the control animals, viral genomic RNA (gRNA) was detected in BAL fluid on all days and
100 viral subgenomic RNA (sgRNA), indicative of virus replication, was detected at 3 and 5 days
101 post inoculation (DPI). In contrast, viral gRNA was detected in only two animals, either on 3 or
102 7 DPI, and no viral sgRNA could be detected in BAL fluid obtained from vaccinated animals
103 ($p=0.0119$, Figure 3b). Viral gRNA was detected in nose swabs from all animals and no
104 difference in viral load in nose swabs was found on any days between vaccinated and control
105 animals (Figure 3c).

106



107

108 **Figure 3. Clinical signs and viral load in rhesus macaques inoculated with SARS-CoV-2**

109 **after vaccination with ChAdOx1 nCoV-19. a.** Mean clinical score with standard deviation in

110 NHPs. Any scoring associated with food was removed from final score. **b.** Viral load in BAL

111 fluid obtained from rhesus macaques, bar at geometric mean. *=p-value < 0.0166. **c.** Viral load in

112 nose swabs obtained from rhesus macaques, bar at geometric mean. **d.** Viral load in tissues at 7

113 DPI. Pictured are individual values with geometric mean bars (left panels) and geometric mean

114 of all lung lobes per group (right panel). ***=p-value < 0.001; ****=p-value < 0.0001. Vaccinated

115 animals = red circles; control animals = blue squares; dotted line = limit of detection.

116

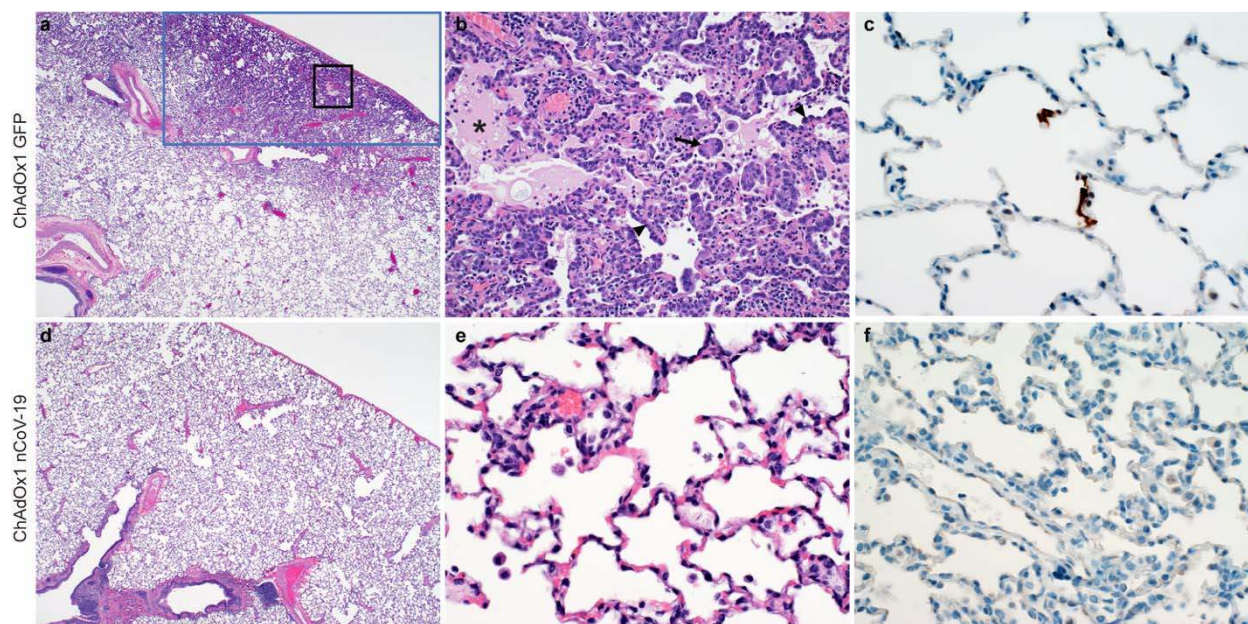
117 **Cytokine response**

118 Cytokines in serum were analysed after challenge to monitor immune responses. We observed an
119 upregulation in IFN- γ at 1 DPI in ChAdOx1 nCoV-19 vaccinated animals, but not in control
120 animals. No significant differences were observed between ChAdOx1 nCoV-19 and control
121 animals for TNF- α , IL-2, IL-4, IL-6, and IL-10 (Extended Data Figure 2).

122

123 **Pulmonary pathology**

124 At 7 days post inoculation, all animals were euthanized, and tissues were collected. None of the
125 vaccinated monkeys developed pulmonary pathology after inoculation with SARS-CoV-2. All
126 lungs were histologically normal and no evidence of viral pneumonia nor immune-enhanced
127 inflammatory disease was observed. In addition, no SARS-CoV-2 antigen was detected by
128 immunohistochemistry in the lungs of any of the vaccinated animals. Two out of 3 control
129 animals developed some degree of viral interstitial pneumonia. Lesions were widely separated
130 and characterized by thickening of alveolar septae by small amounts of edema fluid and few
131 macrophages and lymphocytes. Alveoli contained small numbers of pulmonary macrophages
132 and, rarely, edema. Type II pneumocyte hyperplasia was observed. Multifocally, perivascular
133 infiltrates of small numbers of lymphocytes forming perivascular cuffs were observed.
134 Immunohistochemistry demonstrated viral antigen in type I and II pneumocytes, as well as in
135 alveolar macrophages (Figure 4).



136

137 **Figure 4. Histological changes in lungs of rhesus macaques on 7 dpi.** a) Focal interstitial
138 pneumonia in lungs of a control animal (blue box). The area in the black box is magnified in
139 panel b. b) Interstitial pneumonia with edema (asterisk), type II pneumocyte hyperplasia
140 (arrowhead) and syncytial cells (arrow) in control animals. c) SARS-CoV-2 antigen (visible as
141 red-brown staining) was detected by immunohistochemistry in type I and type II pneumocytes in
142 the lungs of control animals. d) No histological changes were observed in the lungs of ChadOx1
143 nCoV-19-vaccinated animals. e) Higher magnification of lung tissue in panel d. No evidence of
144 pneumonia or immune-enhanced inflammation is observed. f) No SARS-CoV-2 antigen was
145 detected by immunohistochemistry in the lungs of vaccinated animals. Magnification: panels a, d
146 40x; panels b, c, e, f 400x.

147

148 **Viral load in respiratory tract**

149 Viral gRNA load was high in lung tissue of control animals and viral sgRNA was detected in 2
150 out of 3 control animals (Figure 3d). In contrast, the viral gRNA load was significantly lower in
151 lung tissue obtained from vaccinated animals as determined via Mann-Whitney's rank test and

152 below limits of detection in two vaccinated animals. Viral sgRNA was detected in lung tissue
153 obtained from 1 out of 6 vaccinated animals ($p < 0.0001$, Figure 3d). Viral gRNA could be
154 detected in other tissues but was low in both groups (Extended Data Figure 3).

155

156 **Discussion**

157 Here, we showed that a single vaccination with ChAdOx1 nCoV-19 is effective in preventing
158 damage to the lungs upon high dose challenge with SARS-CoV-2. Similarly a recent study
159 showed that a triple vaccination regime of a high dose of whole inactivated SARS-CoV-2
160 protected rhesus macaques from SARS-CoV-2 pneumonia⁷.

161 Viral loads in BAL fluid and lung tissue of vaccinated animals were significantly reduced,
162 suggesting that vaccination prevents virus replication in the lower respiratory tract. Despite this
163 marked difference in virus replication in the lungs, reduction in viral shedding from the nose was
164 not observed. However, animals were challenged with a high dose of virus via multiple routes,
165 which likely does not reflect a realistic human exposure. Whether a lower challenge dose would
166 result in more efficient protection of the upper respiratory tract remains to be determined.

167 Several preclinical studies of vaccines against SARS-CoV-1 resulted in immunopathology after
168 vaccination and challenge, with more severe disease in vaccinated animals than in controls⁸⁻¹⁰.

169 Importantly, we did not see any evidence of immune-enhanced disease in vaccinated animals.

170 The immune response was not skewed towards a Th2 response in mice nor in NHPs, there was
171 no increase in clinical signs or virus replication throughout the study in vaccinated NHPs
172 compared to controls and no markers of disease enhancement in lung tissue of NHPs, such as an
173 influx of neutrophils were observed. These data informed the start of the phase I clinical trial
174 with ChAdOx1 nCoV-19 on April 23, 2020. As of May 13, 2020, more than 1000 volunteers

175 have participated in the clinical trials. This study is thus an important step towards the
176 development of a safe and efficacious SARS-CoV-2 vaccine.

177

178 **References**

- 179 1 Zhu, N. *et al.* A Novel Coronavirus from Patients with Pneumonia in China, 2019. *N Engl J Med*
180 **382**, 727-733, doi:10.1056/NEJMoa2001017 (2020).
- 181 2 Wu, F. *et al.* A new coronavirus associated with human respiratory disease in China. *Nature* **579**,
182 265-269, doi:10.1038/s41586-020-2008-3 (2020).
- 183 3 WHO. *Coronavirus disease (COVID-19) Situation Report 113*,
184 <[https://www.who.int/docs/default-source/coronaviruse/situation-reports/20200512-covid-19-](https://www.who.int/docs/default-source/coronaviruse/situation-reports/20200512-covid-19-sitrep-113.pdf?sfvrsn=feac3b6d_2)
185 [sitrep-113.pdf?sfvrsn=feac3b6d_2](https://www.who.int/docs/default-source/coronaviruse/situation-reports/20200512-covid-19-sitrep-113.pdf?sfvrsn=feac3b6d_2)> (2020).
- 186 4 Lurie, N., Saville, M., Hatchett, R. & Halton, J. Developing Covid-19 Vaccines at Pandemic
187 Speed. *N Engl J Med*, doi:10.1056/NEJMp2005630 (2020).
- 188 5 van Doremalen, N. *et al.* A single dose of ChAdOx1 MERS provides protective immunity in
189 rhesus macaques. *Science Advances*, doi:10.1126/sciadv.aba8399 (2020).
- 190 6 Munster, V. J. *et al.* Respiratory disease in rhesus macaques inoculated with SARS-CoV-2.
191 *Nature*, doi:10.1038/s41586-020-2324-7 (2020).
- 192 7 Qiang, G. *et al.* Development of an inactivated vaccine candidate for SARS-CoV-2. *Science*,
193 doi:10.1126/science.abc1932 (2020).
- 194 8 Weingartl, H. *et al.* Immunization with modified vaccinia virus Ankara-based recombinant
195 vaccine against severe acute respiratory syndrome is associated with enhanced hepatitis in ferrets.
196 *J Virol* **78**, 12672-12676, doi:10.1128/JVI.78.22.12672-12676.2004 (2004).
- 197 9 Bolles, M. *et al.* A double-inactivated severe acute respiratory syndrome coronavirus vaccine
198 provides incomplete protection in mice and induces increased eosinophilic proinflammatory
199 pulmonary response upon challenge. *J Virol* **85**, 12201-12215, doi:10.1128/JVI.06048-11 (2011).
- 200 10 Liu, L. *et al.* Anti-spike IgG causes severe acute lung injury by skewing macrophage responses
201 during acute SARS-CoV infection. *JCI Insight* **4**, doi:10.1172/jci.insight.123158 (2019).
- 202

203 **Methods**

204 **Ethics Statement**

205 Mice - Mice were used in accordance with the UK Animals (Scientific Procedures) Act under project
206 license number P9804B4F1 granted by the UK Home Office. Animals were group housed in IVCs under
207 SPF conditions, with constant temperature and humidity with lighting on a fixed light/dark cycle (12-
208 hours/12-hours).

209 NHPs - Animal experiment approval was provided by the Institutional Animal Care and Use Committee
210 (IACUC) at Rocky Mountain Laboratories. Animal experiments were executed in an Association for
211 Assessment and Accreditation of Laboratory Animal Care (AALAC)-approved facility by certified staff,

212 following the basic principles and guidelines in the NIH Guide for the Care and Use of Laboratory
213 Animals, the Animal Welfare Act, United States Department of Agriculture and the United States Public
214 Health Service Policy on Humane Care and Use of Laboratory Animals. Rhesus macaques were housed in
215 individual primate cages allowing social interactions, in a climate-controlled room with a fixed light/dark
216 cycle (12-hours/12-hours) and monitored a minimum of twice daily. Commercial monkey chow, treats,
217 and fruit were provided by trained personnel. Water was available ad libitum. Environmental enrichment
218 consisted of a variety of human interaction, commercial toys, videos, and music. The Institutional
219 Biosafety Committee (IBC) approved work with infectious SARS-CoV-2 virus strains under BSL3
220 conditions. All sample inactivation was performed according to IBC approved standard operating
221 procedures for removal of specimens from high containment.

222 **Generation of vaccine ChAdOx1 nCoV-19**

223 The spike protein of SARS-CoV-2 (Genbank accession number YP_009724390.1), the surface
224 glycoprotein responsible for receptor binding and fusion/entry into the host cell, was codon optimised for
225 expression in human cell lines and synthesised with the tissue plasminogen activator (tPA) leader
226 sequence at the 5' end by GeneArt Gene Synthesis (Thermo Fisher Scientific). The sequence, encoding
227 SARS-CoV-2 amino acids 2-1273 and tPA leader, was cloned into a shuttle plasmid using InFusion
228 cloning (Clontech). The shuttle plasmid encodes a modified human cytomegalovirus major immediate
229 early promoter (IE CMV) with tetracycline operator (TetO) sites, poly adenylation signal from bovine
230 growth hormone (BGH), between Gateway® recombination cloning sites. ChAdOx1 nCoV-19 was
231 prepared using Gateway® recombination technology (Thermo Fisher Scientific) between the shuttle
232 plasmid described and the ChAdOx1 destination DNA BAC vector described in¹¹ resulting in the
233 insertion of the SARS-CoV-2 expression cassette at the E1 locus. The ChAdOx1 adenovirus genome was
234 excised from the BAC using unique PmeI sites flanking the adenovirus genome sequence. The virus was
235 rescued and propagated in T-Rex 293 HEK cells (Invitrogen) which repress antigen expression during
236 virus propagation. Purification was by CsCl gradient ultracentrifugation. Virus titers were determined by
237 hexon immunostaining assay and viral particles calculated based on spectrophotometry^{12,13}.

238 **Study design animal experiments**

239 Mice – Female BALB/cOlaHsd (BALB/c) (Envigo) and outbred CrI:CD1(ICR) (CD1) (Charles River)
240 mice of at least 6 weeks of age, were immunized IM in the musculus tibialis with 6×10^9 VP of ChAdOx1
241 nCoV-19 unless otherwise stated.
242 NHPs - 9 adult rhesus macaques (8M, 1F) were randomly divided into two groups of six and three
243 animals. Group 1 was vaccinated with ChAdOx1 nCoV-19 at -28 DPI, group 2 was vaccinated with
244 ChAdOx1 GFP at -28 DPI. All vaccinations were done with 2.5×10^{10} VP/animal diluted in sterile PBS.
245 Blood samples were obtained before vaccination and 14 days thereafter. Animals were challenged with
246 SARS-CoV-2 strain nCoV-WA1-2020 (MN985325.1) diluted in sterile DMEM on 0 DPI; with
247 administration of 4 mL intratracheally, 1 mL intranasally, 1 mL orally and 0.5 mL ocularly of 4×10^5
248 TCID₅₀/mL virus suspension. Animals were scored daily by the same person who was blinded to study
249 group allocations using a standardized scoring sheet. Clinical exams were performed on -28, -14, 0, 1, 3,
250 and 5 and 7 DPI. Nasal swabs and blood were collected at all exam dates. BAL was performed on 3, 5,
251 and 7 DPI by insertion of an endotracheal tube and bronchoscope into the trachea, then past the 3rd
252 bifurcation, and subsequent installation of 10 mL of sterile saline. Manual suction was applied to retrieve
253 the BAL sample. Necropsy was performed on 7 DPI and the following tissues were collected: cervical
254 lymph node, mediastinal lymph node, conjunctiva, nasal mucosa, oropharynx, tonsil, trachea, all six lung
255 lobes, right and left bronchus, heart, liver, spleen, kidney, stomach, duodenum, jejunum, ileum, cecum,
256 colon, urinary bladder.

257 **Cells and virus**

258 SARS-CoV-2 strain nCoV-WA1-2020 (MN985325.1) was provided by CDC, Atlanta, USA. Virus
259 propagation was performed in VeroE6 cells in DMEM supplemented with 2% fetal bovine serum, 1 mM
260 L-glutamine, 50 U/ml penicillin and 50 µg/ml streptomycin. VeroE6 cells were maintained in DMEM
261 supplemented with 10% fetal bovine serum, 1 mM L-glutamine, 50 U/ml penicillin and 50 µg/ml
262 streptomycin.

263 **Virus neutralization assay**

264 Sera were heat-inactivated (30 min, 56 °C), two-fold serial dilutions were prepared in 2% DMEM and
265 100 TCID₅₀ of SARS-CoV-2 was added. After 1hr incubation at 37 °C and 5% CO₂, virus:serum mixture
266 was added to VeroE6 cells and incubated at 37°C and 5% CO₂. At 5 dpi, cytopathic effect was scored.
267 The virus neutralization titer was expressed as the reciprocal value of the highest dilution of the serum
268 which still inhibited virus replication.

269 **RNA extraction and quantitative reverse-transcription polymerase chain reaction**

270 Tissues (up to 30 mg) were homogenized in RLT buffer and RNA was extracted using the RNeasy kit
271 (Qiagen) according to the manufacturer's instructions. RNA was extracted from BAL fluid and nasal
272 swabs using the QiaAmp Viral RNA kit (Qiagen) according to the manufacturer's instructions. Viral
273 gRNA¹⁴ and sgRNA¹⁵ specific assays were used for the detection of viral RNA. Five µl RNA was tested
274 with the Rotor-Gene™ probe kit (Qiagen) according to instructions of the manufacturer. Dilutions of
275 SARS-CoV-2 standards with known genome copies were run in parallel.

276 **Enzyme-linked immunosorbent assay for mouse sera**

277 MaxiSorp plates (Nunc) were coated with S1 or S2 (The Native Antigen Company; 50 ng/well) in PBS
278 for overnight adsorption at 4°C. Plates were washed in PBS/Tween (0.05% v/v) and wells blocked using
279 casein (ThermoFisher Scientific) for 1hr at RT. Serially diluted mouse serum samples were added and
280 incubated overnight at 4°C. Plates were washed and Alkaline Phosphatase-conjugated goat anti-mouse
281 IgG (Sigma) was added to all wells for 1hr at RT. After washing pNPP substrate (Sigma) was added.
282 Optical density (OD) values for each well were measured at 405 nm. Endpoint titers were calculated as
283 follows: the log₁₀ OD against log₁₀ sample dilution was plotted and a regression analysis of the linear part
284 of this curve allowed calculation of the endpoint titer with an OD of three times the background. The
285 same calculation was used for diluting the sera to the same amounts of total IgG for further testing on
286 different IgG subclasses with anti-mouse IgG subclass-specific antibodies (Abcam). The results of the
287 IgG subclass ELISA are presented using OD values.

288 **Enzyme-linked immunosorbent assay for NHP sera**

289 Stabilized SARS-CoV-2 spike protein was obtained from the Vaccine Research Centre, Bethesda, USA.
290 Maxisorp plates (Nunc) were coated overnight at 4°C with 100 ng/well spike protein in PBS. Plates were
291 blocked with 100 µl of casein in PBS (Thermo Fisher) for 1hr at RT. Serum serially diluted 2x in casein
292 in PBS was incubated at RT for 1hr. Antibodies were detected using affinity-purified polyclonal antibody
293 peroxidase-labeled goat-anti-monkey IgG (Seracare, 074-11-021) in casein and TMB 2-component
294 peroxidase substrate (Seracare, 5120-0047), developed for 5-10 min, and reaction was stopped using stop
295 solution (Seracare, 5150-0021) and read at 450 nm. All wells were washed 4x with PBST 0.1% tween in
296 between steps. Threshold for positivity was set at 3x OD value of negative control (serum obtained from
297 non-human primates prior to start of the experiment) or 0.2, whichever one was higher.

298 **ELISpot assay and ICS analysis**

299 Single cell suspension of murine splenocytes were prepared by passing cells through 70µM cell strainers
300 and ACK lysis prior to resuspension in complete media. Rhesus macaque PBMCs were isolated from
301 ethylene diamine tetraaceticacid (EDTA) whole blood using Leucosep™ tubes (Greiner Bio-one
302 International GmbH) and Histopaque®-1077 density gradient cell separation medium (Sigma-Aldrich)
303 according to the manufacturers' instructions.

304 Mice - For analysis of IFN-γ production by ELISpot, cells were stimulated with pools of S1 or S2
305 peptides (final concentration of 2µg/ml) on IPVH-membrane plates (Millipore) coated with 5µg/ml anti-
306 mouse IFN-γ (AN18). After 18-20 hours of stimulation, IFN-γ spot forming cells (SFC) were detected by
307 staining membranes with anti-mouse IFN-γ biotin (1µg/ml) (R46A2) followed by streptavidin-Alkaline
308 Phosphatase (1µg/ml) and development with AP conjugate substrate kit (BioRad, UK).

309 For analysis of intracellular cytokine production, cells were stimulated at 37°C for 6 hours with 2µg/ml S1
310 or S2 pools of peptide, media or cell stimulation cocktail (containing PMA-Ionomycin, Biolegend),
311 together with 1µg/ml Golgi-plug (BD) with the addition of 2µl/ml CD107a-Alexa647. Cell supernatant
312 was collected and frozen at -20°C for subsequent analysis by MesoScaleDiscovery (MSD) assay (see
313 below). Following surface staining with CD4-BUV496, CD8-PerCPCy5.5, CD62L-BV711 and CD127-

314 BV650, cells were fixed with 4% paraformaldehyde and stained intracellularly with TNF- α -A488, IL-2-
315 PECy7, IL-4-BV605, IL-10-PE and IFN- γ -e450 diluted in Perm-Wash buffer (BD).
316 Sample acquisition was performed on a Fortessa (BD) and data analyzed in FlowJo v9 or FlowJo V10
317 (TreeStar). An acquisition threshold was set at a minimum of 5000 events in the live CD3⁺ gate. Antigen
318 specific T cells were identified by gating on LIVE/DEAD negative, doublet negative (FSC-H vs FSC-A),
319 size (FSC-H vs SSC), CD3⁺, CD4⁺ or CD8⁺ cells and cytokine positive. Cytokine positive responses are
320 presented after subtraction of the background response detected in the corresponding unstimulated sample
321 (media containing CD107a and Golgi-plug) of each individual spleen sample.
322 NHPs - IFN- γ ELISpot assay of PBMCs was performed using the ImmunoSpot® Human IFN- γ Single-
323 Color Enzymatic ELISpot Assay Kit according to the manufacturer's protocol (Cellular Technology
324 Limited). PBMCs were plated at a concentration of 100,000 cells per well and were stimulated with four
325 contiguous peptide pools spanning the length of the SARS-CoV-2 spike protein sequence at a
326 concentration of 2 μ g/mL per peptide (Mimotopes). ELISpot plates were subjected to overnight formalin
327 inactivation prior to removal from BSL4 for reading. Analysis was performed using the CTL
328 ImmunoSpot® Analyzer and ImmunoSpot® Software (Cellular Technology Limited). Spot forming units
329 (SFU) per 1.0×10^6 PBMCs were summed across the 4 peptide pools for each animal.

330 **Measurement of cytokines and chemokines**

331 Mouse samples were assayed using MSD Technology V-PLEX Mouse Cytokine 29-Plex kit according to
332 the manufacturer's instructions. Non-human primate samples were inactivated with γ -radiation (2 MRad)
333 according to standard operating procedures and assayed on a Bio-Plex 200 instrument (Bio-Rad) using the
334 Non-Human Primate Cytokine MILLIPLEX map 23-plex kit (Millipore) according to the manufacturer's
335 instructions. LLOD was used for all undetectable and extrapolated values. Only data for cytokines
336 consistently above the lower limit of quantification were included in further analyses.

337 Log₁₀ Fold Change (Log₁₀FC) for mouse samples was calculated as follows:

$$338 \text{Log}_{10}\text{FC} = \text{Log}_{10}((\text{Stimulated (pg/ml)} + 1) / (\text{Unstimulated (pg/ml)} + 1))$$

339 Fold change for NHP samples was calculated as follows:

340 $FC = \text{Concentration (pg/mL) on DX (1, 3, 5, or 7)} / \text{Concentration (pg/mL) on D0}$

341 **Histology and immunohistochemistry**

342 Necropsies and tissue sampling were performed according to IBC-approved protocols. Lungs were
343 perfused with 10% formalin and processed for histologic review. Harvested tissues were fixed for eight
344 days in 10% neutral-buffered formalin, embedded in paraffin, processed using a VIP-6 Tissue Tek
345 (Sakura Finetek, USA) tissue processor, and embedded in Ultraffin paraffin polymer (Cancer Diagnostics,
346 Durham, NC). Samples were sectioned at 5 μm , and resulting slides were stained with hematoxylin and
347 eosin. Specific anti-CoV immunoreactivity was detected using an in-house SARS-CoV-2 nucleocapsid
348 protein rabbit antibody (Genscript) at a 1:1000 dilution. The IHC assay was carried out on a Discovery
349 ULTRA automated staining instrument (Roche Tissue Diagnostics) with a Discovery ChromoMap DAB
350 (Ventana Medical Systems) kit. All tissue slides were evaluated by a board-certified veterinary anatomic
351 pathologist blinded to study group allocations.

352 **Statistical analyses**

353 Two-tailed Mann-Whitney's rank tests were conducted to compare differences between groups. A
354 Bonferroni correction was used to control for type I error rate where required.

355 **Data availability**

356 Data have been deposited in Figshare: 10.6084/m9.figshare.12290696

357

358 **References**

- 359
- 360 11 Dicks, M. D. *et al.* A novel chimpanzee adenovirus vector with low human seroprevalence:
361 improved systems for vector derivation and comparative immunogenicity. *PLoS One* **7**, e40385,
362 doi:10.1371/journal.pone.0040385 (2012).
 - 363 12 Bewig, B. & Schmidt, W. E. Accelerated titering of adenoviruses. *Biotechniques* **28**, 870-873,
364 doi:10.2144/00285bm08 (2000).
 - 365 13 Maizel, J. V., Jr., White, D. O. & Scharff, M. D. The polypeptides of adenovirus. I. Evidence for
366 multiple protein components in the virion and a comparison of types 2, 7A, and 12. *Virology* **36**,
367 115-125, doi:10.1016/0042-6822(68)90121-9 (1968).
 - 368 14 Corman, V. M. *et al.* Detection of 2019 novel coronavirus (2019-nCoV) by real-time RT-PCR.
369 *Euro Surveill* **25**, doi:10.2807/1560-7917.ES.2020.25.3.2000045 (2020).

370 15 Wolfel, R. *et al.* Virological assessment of hospitalized patients with COVID-2019. *Nature*,
371 doi:10.1038/s41586-020-2196-x (2020).

372

373 **Acknowledgements**

374 The authors would like to acknowledge Olubukola Abiona, Brandon Bailes, Aaron Carmody, Kizzmekia
375 Corbett, Kathleen Cordova, Jayne Faris, Heinz Feldmann, Susan Gerber, Barney Graham, Elaine
376 Haddock, Ryan Kissinger, Michael Jones, Mary Marsh, Kay Menk, Anita Mora, Stephanie Seifert, Les
377 Shupert, Brian Smith, Natalie Thornburg, Amanda Weidow, Marissa Woods, and Kwe Claude Yinda for
378 their contributions to this study. This work was supported by the Intramural Research Program of the
379 National Institute of Allergy and Infectious Diseases (NIAID), National Institutes of Health (NIH)
380 (1ZIAAI001179-01) and the Department of Health and Social Care using UK Aid funding managed by
381 the NIHR.

382

383 **Author Information**

384 **Author contributions**

385 NvD, TL, SG and VJM designed the study; NvD, TL, AS, SBR, JNP, JRP, VA, TB, AF, MU, FF, EA,
386 HS, JS, MH, AO, KMW, LPP, CB, CG, BNW, RR, DL, AI, RK, LR, SM, CP, JL, PH, DS, GS, EdW,
387 SG, VJM acquired, analysed and interpreted the data; NvD, TL, EdW, SG, and VJM wrote the
388 manuscript. All authors have approved the submitted version.

389 **Corresponding author**

390 Correspondence to Vincent Munster, vincent.munster@nih.gov or Sarah Gilbert,

391 sarah.gilbert@ndm.ox.ac.uk

392

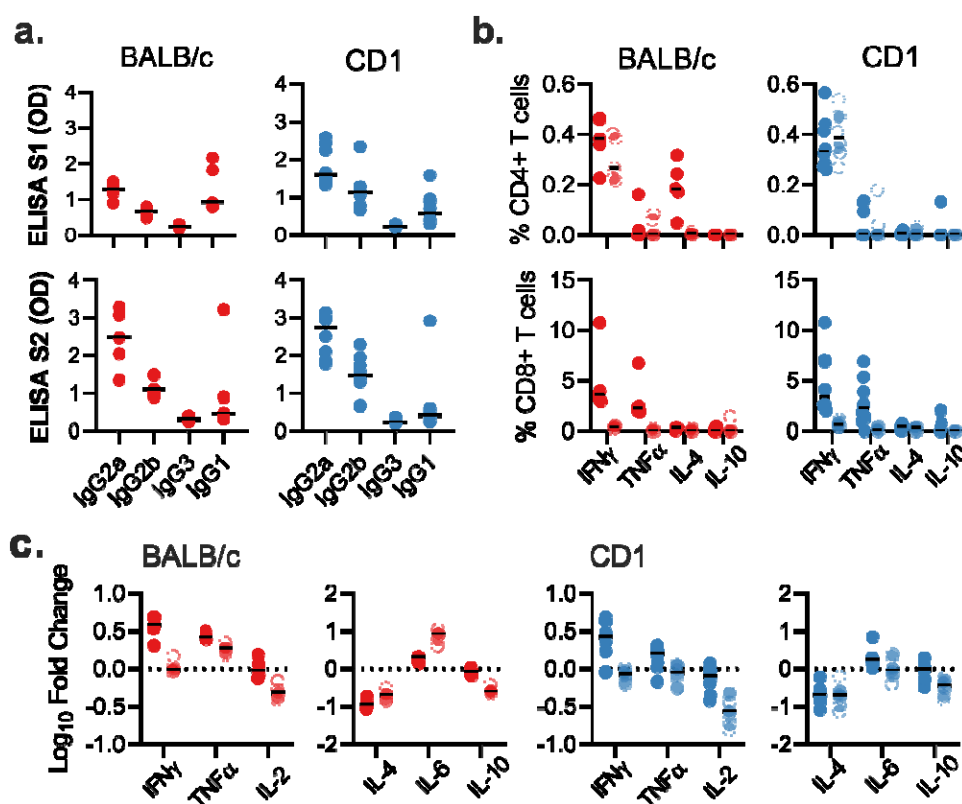
393 **Competing interests**

394 SCG is a board member of Vaccitech and named as an inventor on a patent covering use of ChAdOx1-
395 vectored vaccines and a patent application covering a SARS-CoV-2 (nCoV-19) vaccine. Teresa Lambe is

396 named as an inventor on a patent application covering a SARS-CoV-2 (nCoV-19) vaccine. The remaining
397 authors declare no competing interests.

398

399 Extended Data Legends



400

401 Extended Data Figure 1. Antigen specific responses following ChAdOx1 nCov19

402 vaccination.

403 a. IgG subclass antibodies detected against S1 or S2 protein in sera of BALB/c or CD1 mice. b.

404 Frequency of cytokine positive CD4+ or CD8+ T cells following stimulation of splenocytes with

405 S1 pool (dark) or S2 pool (transparent) peptides in BALB/c (red) and CD1 (blue) mice. d. Log₁₀

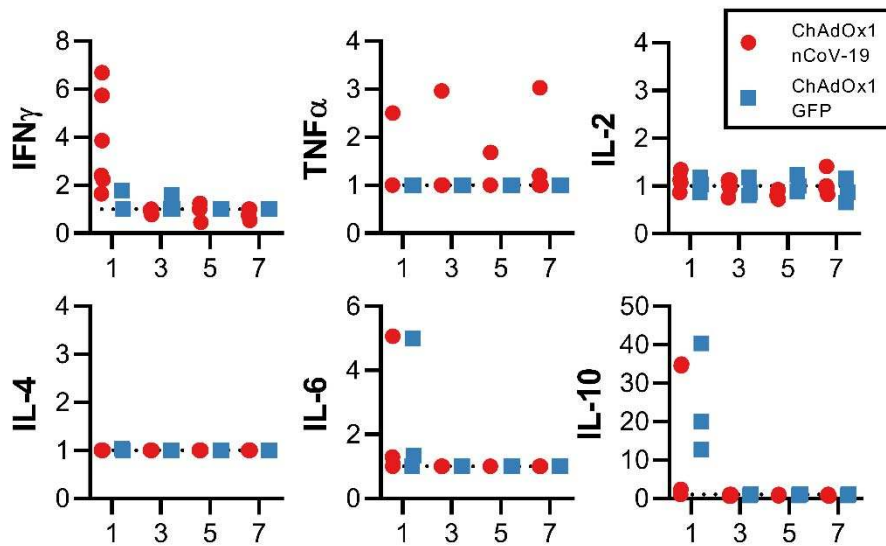
406 fold change in cytokine levels in supernatant from S1 (dark) and S2 (transparent) stimulated

407 splenocytes when compared to corresponding unstimulated splenocyte sample for BALB/c and
408 CD1 mice.

409 **Extended Data Table 1. Clinical signs observed in rhesus macaques inoculated with SARS-CoV-2**

Animal	Treatment	D0	D1	D2	D3	D4	D5	D6	D7
1	Vaccine	Normal	Normal	Normal	Normal	Normal	Normal	Normal	Normal
2	Vaccine	Normal	Normal	Dyspnea with abdominal effort	Dyspnea with abdominal effort	Normal	Normal	Normal	Normal
3	Vaccine	Normal	Normal	Dyspnea with abdominal effort	Dyspnea with abdominal effort	Dyspnea with abdominal effort	Normal	Normal	Normal
4	Vaccine	Normal	Normal	Tachypnea	Tachypnea	Tachypnea	Tachypnea	Tachypnea	Normal
5	Vaccine	Normal	Tachypnea	Tachypnea	Tachypnea	Tachypnea	Normal	Normal	Normal
6	Vaccine	Normal	Ruffled fur	Tachypnea, ruffled fur	Tachypnea, ruffled fur	Tachypnea, ruffled fur	Normal	Normal	Normal
7	Control	Normal	Normal	Diarrhoea	Tachypnea, ruffled fur, diarrhoea	Dyspnea, ruffled fur, diarrhoea, red nose	Dyspnea, diarrhoea	Normal	Normal
8	Control	Normal	Dyspnea	Tachypnea	Tachypnea, pale appearance	Tachypnea, pale appearance	Tachypnea	Tachypnea	Tachypnea
9	Control	Normal	Dyspnea	Tachypnea, ruffled fur	Tachypnea, ruffled fur	Tachypnea, ruffled fur	Tachypnea	Tachypnea	Tachypnea

410

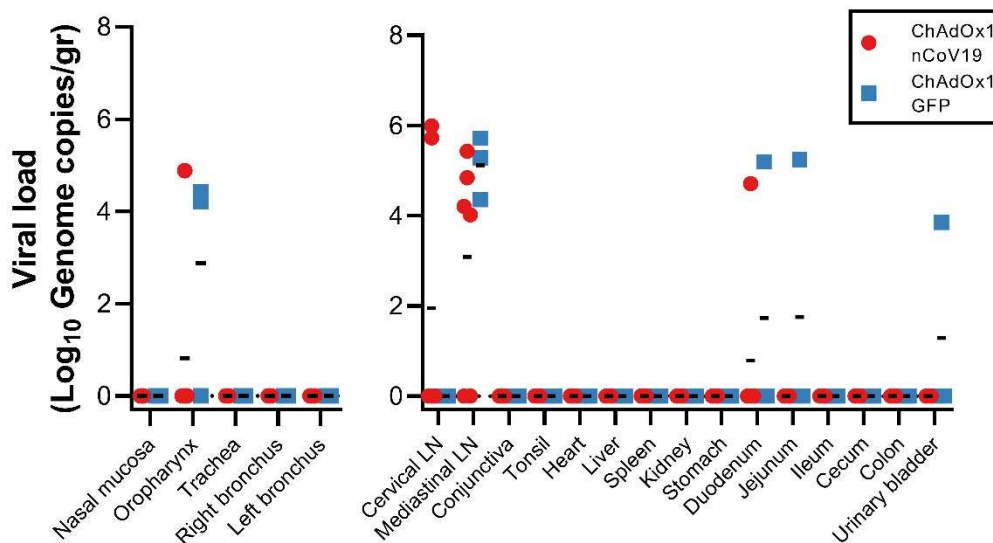


411

412 **Extended Data Figure 2. Serum cytokines in rhesus macaques challenged with SARS-CoV-2. Fold**

413 increase in cytokines in serum compared to 0 DPI values.

414



415

416 **Extended Data Figure 3. Viral load in rhesus macaques challenged with SARS-CoV-2**

417 Viral genomic RNA in respiratory tissues excluding lung tissue (left panel) and other tissues (right panel).

418 A two-tailed Mann-Whitney's rank test was performed to investigate statistical significance. Bonferroni

419 correction was applied, and thus statistical significance was reached at $p > 0.0125$.